Proceedings of the 21st ICSMGE, Vienna, Austria, 14 – 19 June 2026. Pistrol, Adam & Schweiger (eds.)
Published by: ÖGG, Austrian Society for Geomechanics, Salzburg, Austria, ISBN 978-3-9503898-4-5
https://doi.org/10.53243/ICSMGE2026-616

Performance prediction of track granular materials using machine learning approaches with an emphasis on input parameter selection

Rakesh Sai Malisetty, Buddhima Indraratna, Srinivas Alagesan, Haydn Hunt, Yujie Qi
Transport Research Centre, University of Technology Sydney, Australia, rakeshsai.malisetty@uts.edu.au

Tim Neville
Australian Rail Transport Corporation, Australia

ABSTRACT: The strength and degradation of track granular layers such as ballast and capping directly influences the condition of railway track affecting its operational efficiency. In recent times, machine learning (ML) models have demonstrated their effectiveness in predicting the engineering properties of geotechnical materials while surpassing complexities in conventional approaches. Despite this progress, the process of selecting appropriate input parameters for these models is not clearly highlighted, which limits their applicability in decision-making. This study aims to address this gap by identifying the optimal set of input parameters for granular materials in railway tracks, utilizing existing data from laboratory testing. The study focuses on two key applications predicting: (i) the peak friction angle (ϕ'_{peak}) of natural and composite granular mixtures subjected to static loading and (ii) particle breakage of ballast under cyclic loading. The optimization process is based on the relevance of input parameters in practice, compliance of ML models with fundamental principles as well as their influence on prediction accuracy. The results revealed that all ML models consistently identified a similar set of optimal input parameters that capture essential information about stress state, gradation characteristics and material composition. While insufficient parameters caused loss of accuracy due to missing critical information, excessive parameters also impeded accuracy due to redundancy-induced bias. Furthermore, evaluating model performance metrics indicated that ANN outperformed other methods with a higher R^2 and lower error, and effectively captured the underlying non-linear relationships between input parameters, ϕ'_{peak} and particle breakage. The advantages of these models are discussed in relevance to enhancing the understanding of track granular material behavior where repeating laboratory experiments becomes cumbersome.

KEYWORDS: Machine learning, granular materials, friction angle, ballast, particle breakage

1 INTRODUCTION

The 21st century developments across the world have necessitated efficient railway transportation systems for both passenger and freight traffic. While some parts of the world use both slab and ballasted tracks for passenger networks, the heavy-haul freight transportation networks across the world are still operated on ballasted railway tracks. The performance of these tracks is majorly dependent on the shear strength and degradation characteristics of granular layers such as ballast and capping to be able to withstand the repetitive heavy loads imparted by trains. For effective performance of these layers, it is important for the granular materials to have sufficient shear strength in both the design phase and during operation. As the prominence of recycling and reusing granular wastes originating from mining and industrial sectors has increased, the variability in shear strength of these materials has also increased due to varied rigidness of waste aggregates (Arulrajah et al., 2014, Indraratna et al., 2018). A few notable examples include rubber-intermixed ballast stratum (RIBS) as alternative to ballast (Arachchige et al., 2022), rubber-sand mixtures (Sheikh et al., 2013) and rubber-waste mixtures which were used as alternative to sub-ballast materials (Qi et al., 2018, Tawk and Indraratna, 2021, Indraratna et al., 2025). Also, under repeated train loading, the peak friction angle (ϕ'_{peak}) of conventional ballast layer is found to reduce with loading cycles due to breakage of larger and angular aggregates into finer particles (Indraratna et al., 2001, Indraratna et al., 2024a, 2024b). In Australian railway tracks, ballast cleaning and replacement accounts for a major amount of maintenance costs every year (Economics, 2022).

Laboratory investigations underlined that the parameters affecting strength and degradation of granular materials can be divided into three categories: (i) soil stress state such as confining stress, loading magnitude and frequency, (ii) soil physical state such as initial void ratio and compaction density, and (iii) soil/rock type such as gradation characteristics and origin material. In the past, empirical models have been developed for predicting the shear strength of conventional subballast materials (Hunt et al., 2023), as well as ballast breakage index (Lackenby et al., 2007, Hussaini and Sweta, 2020), based on data trends from laboratory investigations. However, most of these models are based on only a few selected influential parameters, while their application is often limited to a specific soil type due to specific empirical coefficients. Some constitutive models (Einav, 2007, Malisetty et al., 2020a, Malisetty et al., 2020b) are also available for predicting the peak friction angle of granular materials and its reduction with repeated loading; however, it is much more complex to implement these models incorporating all influential parameters. Machine Learning models in recent years have gained attention with their ability to uncover the hidden relationships in complex datasets. Artificial Neural Networks (ANN) is the most popular ML technique widely used for geotechnical engineering applications. Some examples include prediction models for constitutive behavior of geomaterials (Shahin and Indraratna, 2006, Penumadu and Zhao, 1999), bearing capacity of shallow and pile foundations (Chan et al., 1995, Shahin et al., 2002) and resilient modulus of railway ballast (Indraratna et al., 2023a).

Considering the above, this paper discusses predictive models based on ANN for (a) peak friction angle of subballast materials including recycled wastes, and (b) the evolution of ballast degradation quantified by ballast breakage index. It has been reported by Phoon and Zhang (2023) that the identification and selection of the optimum set of input parameters is imperative for superior performance of ML models and their ability to assist in real-world decision making. In most geotechnical engineering applications, it is not always possible to obtain complete information on all parameters from the field. For this reason, the analysis in this paper specifically focusses on investigating the advantages and shortcomings of including and excluding different input parameters and their influence on the predictive and generalization capability of the model.

2 ANN ARCHITECTURE

A typical ANN consists of three interconnected layers categorized as input, hidden/intermediate and output layers, though some ANNs may have multiple hidden layers depending on the quantity and complexity of data. The hidden layer consists of multiple nodes which act as bridges between input and output layers. The information from the input layer is transferred to the hidden layer through weighting coefficients, which is then summed along with an additional bias and propagated to the output layer through a transfer function. After the predicted output is compared with the measured output, the net loss is then backpropagated, where the weights and bias are updated with the help of a training algorithm (optimization) through an iterative process until the error is less than the desired threshold. For this study, sigmoid function and hyperbolic tangent functions were used as activation functions for input-hidden layer and hidden-output layer interfaces, respectively. Also, the Levenberg-Marquardt (LM) algorithm was used for network optimization.

The overall database was divided into training and testing datasets with a ratio of 80:20. Although the testing set contains unseen data from the ANN model's perspective, it is still related to the data used in the training phase since the same studies and material types were divided across both datasets. Therefore, a completely external set of data that is independent of the original database was also used for external validation. For quantifying the model performance, five evaluation metrics are employed which are the mean absolute relative error (MARE), root mean squared error (RMSE), coefficient of determination ($R2$), variance accounted for (VAF), and A-10 indices as shown in Eqs. 1a to 1e.

$$\text{MARE} = \frac{1}{n}\sum_{i=1}^{n}\frac{|y_p - y_t|}{o_m} \text{ x } 100\% \quad (1a)$$

$$\text{RMSE} = \sqrt{\frac{1}{n}\sum_{i=1}^{n}\left(y_p - y_t\right)^2} \quad (1b)$$

$$R^2 = 1 - \frac{\sum_{i=1}^{n}\left(y_p - y_t\right)^2}{\sum_{i=1}^{n}(\overline{y_t} - y_t)^2} \quad (1c)$$

$$\text{VAF} = \left(1 - \frac{var(y_p - y_t)}{var(y_t)}\right) \times 100\% \quad (1d)$$

$$\text{A-10} = \frac{m10}{n} \quad (1e)$$

where y_p and y_t are the predicted and target output values, respectively; $\overline{y_t}$ is the average of the target values; n is the total number of data samples; var refers to variance; $m10$ are the number of samples where y_p is within $\pm 10\%$ of y_t.

3 FRICTION ANGLE MODEL

3.1 *Database Preparation*

In this section, a predictive model that is capable of accurately predicting ϕ'_{peak} for a variety of track granular materials is discussed. The database considered for this model consists of both conventional granular materials (ballast, subballast and sand) and waste materials (steel furnace slag, SFS; coal wash, CW; and rubber granules), and mixtures of both. A total of 154 consolidated drained static triaxial tests using the above-mentioned materials were adopted from the literature as shown in Table 1. For accurately capturing the influence of waste granules on the shear strength of the overall mixtures, 85% of the database was populated using test data comprised of waste mixtures.

A careful review of past experimental investigations was conducted to identify the input parameters that affect ϕ'_{peak}. As highlighted in Tawk and Indraratna (2021), Hunt et al. (2023) and Indraratna et al. (1998), the non-linearity of the shear failure envelope depends on the effective confinement of the material, whose influence is dominant when marginal materials are used. Hence, the effective confining stress (σ'_3) was considered as a key input representing the initial stress state. In addition to the dry unit weight of the material, the void ratio is also considered as an input in order to account for weight discrepancy when using softer waste materials such as coal wash and rubber granules/crumbs. Gravimetric rubber content (RC%) was included as an input as it was found to affect the peak friction angle. To account for gradation characteristics, five parameters are used which include: coefficient of uniformity (C_u) and curvature (C_c), and effective (D_{10}), mean (D_{50}) and maximum (D_{max}) particle size of the mixtures. The statistics of input parameters are shown in Table 2.

The database was divided into training and testing sets using a semi-random trial-and-error approach ensuring consistent statistics (mean, standard deviation, minimum, and maximum) across all ten variables. Also, care was taken to ensure each material type is included in both testing and training datasets to reduce error.

Table 1. Database for peak friction angle model

Material	Tests Without Rubber	Tests With Rubber	References
Ballast	17	9	Arachchige et al. (2022) Indraratna et al. (1998)
Sand	7	59	Edincliler et al. (2012) Sheikh et al. (2013) Noorzad and Raveshi (2017)
SFS	4	0	Tasalloti (2015)
CW	21	11	Tasalloti (2015) Kaliboullah (2016) Indraratna et al. (2019) Tawk and Indraratna (2021)
SFS-CW	15	11	Tasalloti (2015) Qi et al. (2018)

Table 2. Database statistics for peak friction angle model

Variable	Min-Max	Mean	Std. Dev.
$RC\%$	0-40	9.5	11.3
σ'_3 (kPa)	8-483	102.2	97.4
e_0	0.29-0.88	0.57	0.17
γ_d (kN/m3)	9.1-20.4	14.96	2.1
C_u	1.5-83.1	16.9	23.8
C_c	0.9-4.1	1.6	0.90
D_{10} (mm)	0.013-27.1	3.6	7.7
D_{50} (mm)	0.19-38.9	6.6	12.2
D_{max} (mm)	0.30-53	15.0	18.6
ϕ'_{peak}	26.4-66.5	44.9	8.1

3.2 *Performance evaluation*

For determining the optimum number of nodes in the hidden layer, the performance of ϕ'_{peak} model was evaluated for each configuration with the number of nodes varying from 1-16, from which the best-performing model was selected as elucidated in Indraratna et al. (2025). A ranking system was adopted based on Zorlu et al. (2008) where each network is ranked based on its score with respect to the 5 metrics. It was found that when all 9 input parameters were considered, 8 nodes in the hidden layer yielded best performance during training and testing phases. To improve model's generalization ability, external data from Disfani et al. (2017) and Indraratna et al.

(2018) using mixtures of fine recycled glass and rubber crumbs (FRG-RC) and traditional subballast (crushed rock), respectively, under CD static triaxial compression was used. Interestingly, when the models were evaluated along with the external datasets, the 10 hidden layer model performed better than the model with 8 nodes. The metrics for the 9-10-1 (9 inputs-10 hidden nodes-1 output) model are shown in Table 3, while the plots of predicted vs. measured values of ϕ'_{peak} for the 9-10-1 model are shown in Figures 1a and c, for training and testing, as well as external validation database, where most predictions fall within 10% error.

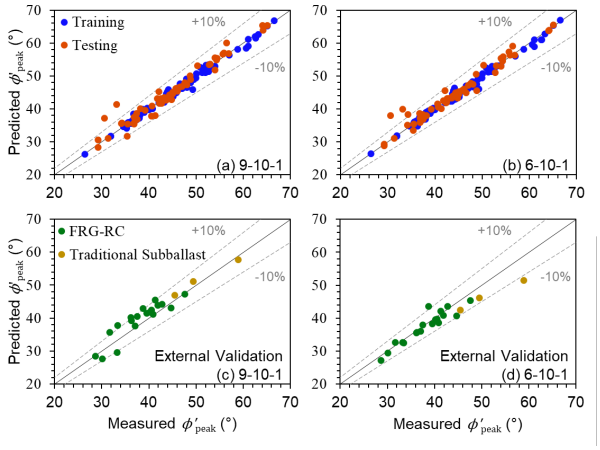

Figure 1. Predicted vs. target peak friction angle values for 9-10-1 and 6-10-1 models with (a,b) original database and (c,d) external data (modified after Indraratna et al. 2025)

Although a larger model that includes all influential parameters is fundamentally ideal, it may not be the best-performing model as some input parameters may have interdependence and thus create errors due to redundancy. Also, in practice, fewer input parameters mean lower human error while measuring those parameters on field. For this purpose, the 5- and 6- input variable models are developed and compared with the 9-10-1 model. The 5-input model includes σ'_3, $RC\%$, e_0, γ_d and D_{50}, while the 6-input model has C_c as an additional parameter. It was ensured that atleast one parameter from each category was included as discussed earlier. Although C_u is reportedly found to influence the peak friction angle, including it resulted in lower accuracy due to its high coefficient of variance within the dataset considered. Also, D_{max} was ignored as it becomes redundant after considering e_0 and γ_d. The same procedure was followed to identify the best number of nodes in hidden layer.

The performance of the 5-7-1 and 6-10-1 models are compared with the 9-10-1 model and the metrics are shown in Table 3. It was observed that the 5-7-1 model performed to a similar capacity as that of 9-10-1 model, though the former model only considers around half of the input parameters as the latter. Furthermore, including C_c resulted in the 6-10-1 model performing better than the other two models, with greater accuracy across all training, testing and external validation datasets. Figures 1c and d show the predicted vs. measured output plots for the 6-10-1 model, which clearly shows far more accuracy in predictions, especially for external data. This proves that careful selection (inclusion and exclusion) of input parameters via geotechnical domain knowledge can help to remove redundancy-related errors, thus improving a model's predictive capability.

Table 3. Performance metrics for peak friction angle model

Model		5-7-1	6-10-1	9-10-1
R^2	Train	0.97	0.99	0.99
	Test	0.94	0.94	0.94
	Ext.	0.83	0.9	0.89
RMSE	Train	1.27	0.85	0.89
	Test	2.46	2.41	2.52
	Ext.	2.8	2.44	2.69
MARE (%)	Train	2	1.3	1.5
	Test	4	4.1	4.4
	Ext.	5.2	4	6.2
VAF (%)	Train	97.3	98.8	98.7
	Test	94	94	93.3
	Ext.	79.1	88.8	88.9
A-10	Train	1	1	1
	Test	0.968	0.903	0.903
	Ext.	0.864	0.909	0.727
Final Score		91	113	86
Rank		2	1	3

4 BALLAST DEGRADATION PREDICTION MODEL

In this section, the ANN framework is used to develop a predictive model for particle breakage of ballast under repeated loading conditions. For this purpose, ballast breakage index (BBI) developed by Indraratna et al. (2005) is used, which is evaluated based on the difference in the area between the PSD curves before and after loading.

Table 4. Database for BBI prediction during training and validation

Stage	**Parent rock**	**References**
Training	Latite basalt	Lackenby et al. (2007); Tennakoon and Indraratna (2014); Hussaini et al. (2016); Indraratna et al. (2016); Sun et al. (2016); Navaratnarajah and Indraratna (2017); Jayasuriya et al. (2019); Arachchige et al. (2022), Ngo et al. (2022), Indraratna et al. (2023b)
Validation	Limestone	Aursudkij et al. (2009)
	Quartzite	Nålsund (2010)
	Basalt	Nimbalkar and Indraratna (2016)
		Sun and Zheng (2017)
	Granite	Hussaini and Sweta (2020)

4.1 *Database Preparation*

The database considered in this paper includes 78 data samples adopted from previous laboratory investigations using large-scale cylindrical triaxial and cubical triaxial apparatus as shown in Table 4. As the evaluation of BBI requires completely stopping a test and conducting sieve analysis, the number of data points is limited. For example, for acquiring a single data point corresponding to BBI at N = 100,000 cycles under specific loading and gradation conditions, the test has to be conducted till 100,000 cycles, after which it has to be restarted for another data point. For such smaller datasets, it is even more important to analyse the influence of the number of input parameters to minimize the number of connection weights (Rogers and Dowla, 1994).

Table 5. Statistical distribution of inputs and outputs for BBI model

	Cylindrical triaxial tests		Cubical triaxial tests	
	Min-Max	Mean/SD	Min Max	Mean Std. Dev.
N	1000 500000	464172 126610	5000 500000	337000 2169256
σ_3' (kPa)	10 240	43.8 32.5	7 20	13.4 3.6
q_{max} (kPa)	230 370	249.3 48.7	230 460	301 99.4
f (Hz)	5 65	24.7 12.4	15 25	17 3.4
D_{max} (mm)	53	53 0	53 63	62.5 2.2
D_{50} (mm)	27.2 49.4	38.8 4.3	33.5 43	35.8 3.2
C_u	1.2 4.5	1.9 0.70	1.6 2.5	1.9 0.42
C_c	1.0 1.4	1.1 0.12	1 1.3	1.1 0.13
γ_dkN/m3)	15.0 15.6	15.3 0.1	15.2 15.3	15.3 0
e_o	0.53 0.82	0.73 0.05	0.72 0.77	0.74 0.02
BBI (%)	1.2 17.7	6.6 3.3	6 13.4	10.3 2.6

Similar to the ϕ'_{peak} model, the parameters are selected based on their category. Since the BBI model contains data from cyclic loading tests, the magnitude of cyclic deviatoric stress (q_{max}), loading frequency (f) and number of loading cycles (N) are also considered along with the effective confining stress. Other parameters include γ_d, e_0, C_u, C_c, D_{50} and D_{max}. A natural logarithmic of the number of loading cycles was used for modelling to avoid model overfitting caused by larger values. Table 5 shows the statistical distribution of the parameters for BBI model. Also, it was observed during data collection that the BBI values differed slightly when the type of apparatus is changed from cylindrical to cubical triaxial apparatus due to the apparent boundary conditions of the sample (Indraratna and Salim, 2003). To account for this difference, a binary input was considered for analysis recognizing the source of the data: 0 for cubical triaxial and 1 for cylindrical triaxial tests. It is to be noted that most of the test data available is related to latite basalt aggregates with a uniaxial compressive strength of 130 kPa (Indraratna et al., 1998), while only limited datasets on ballast made from other rock types (granite, limestone and quartz) are available. To avoid confusion for the model during training, the datasets for training and testing were limited to that of latite basalt aggregates, while data from other rock types are used during external validation. 80:20 ratio was followed for training-testing data division, while keeping same activation functions and training algorithm as the ϕ'_{peak} model.

4.2 *Performance evaluation*

For the BBI model, the input parameters were grouped into 20 different combinations, through a forward selection process based on the Spearman Correlation Coefficient (SCC) as detailed in Indraratna et al. (2025). This selection process starts with 2 input parameters to 9 input parameters, repeated for each binary input. Based on SCC, loading conditions were given first priority, followed by PSD and initial state parameters as shown in Table 5. A 10-noded single hidden layer was adopted, while all the input combinations are compared.

Table 6. Input parameter combinations for BBI model

Groups	Inputs
Group 1A	q_{max}, f
Group 1B	q_{max}, f, σ_3'
Group 1C	q_{max}, f, σ_3', N
Group 1D	$q_{max}, f, \sigma_3', N, D_{50}$
Group 1E	$q_{max}, f, \sigma_3', N, D_{50}, C_c$
Group 1F	$q_{max}, f, \sigma_3', N, D_{50}, C_u$
Group 1G	$q_{max}, f, \sigma_3', N, D_{50}, C_u, C_c$
Group 1H	$N, \sigma_3', q_{max}, f, D_{50}, C_u, C_c, \gamma_d$
Group 1I	$N, \sigma_3', q_{max}, f, D_{50}, C_u, C_c, e_o$
Group 1J	$N, \sigma_3', q_{max}, f, D_{50}, C_u, C_c, \gamma_d, e_o$
Group 2 (A to J)	In Group 2, DT (binary input) is added to the ANN model

Figure 2 shows the mean squared error of the models A-J with (Group-2) and without binary input (Group-1). Lower number of input parameters showed higher MSE due to insufficient information, while MSE improved with increasing the number of inputs. The inclusion of PSD parameters reduced the error by about 30%, while it was observed that including both C_u and C_c parameters improved the BBI model's performance. After including initial state parameters such as γ_d and e_0, the performance of the model reached a plateau with no or little improvement in MSE. Also, it was observed that the best performing model was the ones corresponding to combination H, where γ_d is the only initial state parameter. Adding e_0 (Combination I and J) negatively affected the model where the MSE slightly increased. This indicates that γ_d in conjunction with PSD parameters are sufficient to capture the influence of initial state on BBI, and addition of e_0 induced redundancy. This is slightly different to the ϕ'_{peak} model, where both γ_d and e_0 were needed for the best model. This is due to the singular type of aggregates in ballast with same specific gravity. On the other hand, the data for ϕ'_{peak} model encompassed materials with different specific gravities, requiring additional parameters to quantify the γ_d-e_0-ϕ'_{peak} relationship. Also, it was observed that including information about test type as binary input improved the model performance across all combinations. This further highlights the importance of careful selection of input parameters. The performance metrics for the two best performing models are shown in Table 7.

Table 7. Comparison of performance of two best performing models for BBI

Model		1H	2H
R^2	Train	0.97	0.97
	Test	0.83	0.90
	Ext.	0.71	0.89
RMSE	Train	0.67	0.64
	Test	0.94	0.70
	Ext.	1.91	1.31
MARE (%)	Train	11.4	9.1
	Test	19.1	13.9
	Ext.	17.9	10.0
VAF (%)	Train	96.8	96.9
	Test	82.5	90.2
	Ext.	65.1	84.3
A-10	Train	0.91	0.93
	Test	0.63	0.69
	Ext.	0.40	0.90
Score		20	39
Rank		2	1

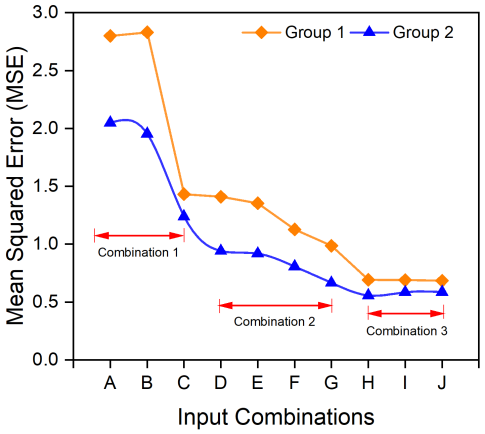

Figure 2. Comparison of MSE for BBI model with different input combinations (modified after Indraratna et al. 2025).

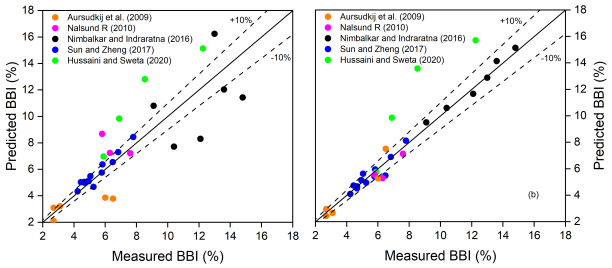

Figure 3. Comparison of model performance - Predicted vs. Measured BBI for (a)1H and (b)2H (modified after Indraratna et al. 2025).

Further, the models 1H and 2H were tested for external datasets, which were completely new for the model. The external database includes datasets on ballast with different types of parent rock as given in Table 4. The data from Nimbalkar and Indraratna (2016) were measured on a real railway track, and for this case, the binary input was considered as 0 similar to cubical triaxial setup, which is more analogous of field conditions. As observed from Figures 3a and b, model 1H's predictions showed errors, with predictions deviating more than 10% consistently for data from all sources. Overall, model 2H yielded an R2 of 0.89 compared to 0.71 for 1H. For latite basalt aggregates, model 2H predicted BBI very close to measured values for both laboratory and field data, increasing confidence on model's applicability to field scenarios.

On the other hand, both 1H and 2H did not do well for ballast aggregates from other parent rock types. This is expected as no additional input informing the model about parent rock type was considered for model development. The RMSE values for quartzite (0.7) and limestone (0.6) aggregates were not very high when compared to that for granite aggregates (3.4). However, without an additional input clearly defining the distinction between input rock types, the current model cannot be confidently used for BBI predictions for rock types other than latite basalt.

5 CONCLUSIONS

This paper presented two data-driven models based on Artificial Neural Networks for predicting the peak static friction angle (ϕ'_{peak}) of track granular materials and ballast breakage index (BBI) under repeated loading conditions. Analysis was conducted to compare models with different input parameter combinations with a key focus on selecting the optimum set of input parameters.

The optimum set of input parameters should include information on all three categories of soil stress state, physical state and type. Considering both an insufficient and excessive number of parameters resulted in increased prediction errors. For the ϕ'_{peak} model, the 6-10-1 combination with 6 input parameters ($RC\%$, σ'_3, e_0, γ_d, D_{50}, C_c) was found to be the best-performing model when compared to a smaller 5-input and a larger 9-input models.

For BBI, the 9-input model is identified as the best performing model (N, q_{max}, f, σ'_3, γ_d, D_{50}, C_u, C_c and binary input). For datasets originating from different types of test setups, including information about the test type, i.e., test boundary conditions, are crucial for accurate prediction of BBI. By considering a binary input to account for this, the 9-input model accurately predicted the BBI measured from Australian railway tracks and other external data sets with an R^2 of 0.87, highlighting the model's capability to be applicable to field data. Overall, with high predictive capability, these models can help to optimise the laboratory testing efforts and make better use of those efforts by highlighting the hidden trends within data.

Although the models were able to predict ϕ'_{peak} and BBI sufficiently, there are still some gaps in the data pertaining to the behaviour of granular materials. For example, the ϕ'_{peak} model does not include information about intermediate principal stress, while the BBI model does not include information about rock type, due to limited data. It is therefore recommended to improve the proposed models with additional inputs and datasets when available in future.

6 ACKNOWLEDGEMENT

The authors express our appreciation for the financial support from the Australian Research Council (LP200200915) and acknowledge the financial and technical assistance from industry partners, including Sydney Trains, Australian Rail Transport Corporation (ARTC), SMEC Australia Pty. Limited, Bentley Systems Pty. Limited, and Bestech Australia Pty. Limited.

7 REFERENCES

Arachchige, C. M. K., Indraratna, B., Qi, Y., Vinod, J. S. & Rujikiatkamjorn, C. 2022. Deformation and degradation behaviour of Rubber Intermixed Ballast System under cyclic loading. *Engineering Geology,* 307**,** 106786.

Arulrajah, A., Ali, M. M. Y., Disfani, M. M. & Horpibulsuk, S. 2014. Recycled-Glass Blends in Pavement Base/Subbase Applications: Laboratory and Field Evaluation. *Journal of Materials in Civil Engineering,* 26**,** 04014025.

Aursudkij, B., Mcdowell, G. & Collop, A. 2009. Cyclic loading of railway ballast under triaxial conditions and in a railway test facility. *Granular Matter,* 11**,** 391.

Chan, W., Chow, Y. & Liu, L. 1995. Neural network: an alternative to pile driving formulas. *Computers and geotechnics,* 17**,** 135-156.

Disfani, M. M., Tsang, H.-H., Arulrajah, A. & Yaghoubi, E. 2017. Shear and compression characteristics of recycled glass-tire mixtures. *Journal of Materials in Civil Engineering,* 29**,** 06017003.

Economics, B. O. 2022. Australian Rail Market Outlook. Australian Railway Association.

Edincliler, A., Cabalar, A. F., Cagatay, A. & Cevik, A. 2012. Triaxial compression behavior of sand and tire wastes using neural networks. *Neural Computing and Applications,* 21**,** 441-452.

Einav, I. 2007. Breakage mechanics—Part II: Modelling granular materials. *Journal of the Mechanics and Physics of Solids,* 55**,** 1298-1320.

Hunt, H., Indraratna, B. & Qi, Y. 2023. Ductility and energy absorbing behaviour of coal wash – rubber crumb mixtures. *International Journal of Rail Transportation,* 11**,** 508-528.

Hussaini, S. K. K., Indraratna, B. & Vinod, J. S. 2016. A laboratory investigation to assess the functioning of railway ballast with and without geogrids. *Transportation Geotechnics,* 6**,** 45-54.

Hussaini, S. K. K. & Sweta, K. 2020. Investigation of deformation and degradation response of geogrid-reinforced ballast based on model

track tests. *Proceedings of the Institution of Mechanical Engineers, Part F: Journal of Rail and Rapid Transit,* 235**,** 505-517.
Indraratna, B., Armaghani, D. J., Correia, A. G., Hunt, H. & Ngo, T. 2023a. Prediction of resilient modulus of ballast under cyclic loading using machine learning techniques. *Transportation Geotechnics,* 38**,** 100895.
Indraratna, B., Hunt, H., Malisetty, R. S., Alagesan, S., Qi, Y. & Rujikiatkamjorn, C. 2025. Optimization of inputs for the application of ANN to rail track granular materials. *Canadian Geotechnical Journal,* 62**,** 1-22.
Indraratna, B., Ionescu, D. & Christie, H. 1998. Shear behavior of railway ballast based on large-scale triaxial tests. *Journal of Geotechnical and Geoenvironmental Engineering,* 124**,** 439-449.
Indraratna, B., Lackenby, J. & Christie, D. 2005. Effect of confining pressure on the degradation of ballast under cyclic loading. *Géotechnique,* 55**,** 325-328.
Indraratna, B., Malisetty, R.S., Arachchige, C., Qi, Y. and Rujikiatkamjorn, C. 2024a. Sustainable Performance of Recycled Rubber and Mining Waste Utilized for Efficient Rail Infrastructure. *Indian Geotechnical Journal*, **54**, 1738–1750.
Indraratna, B., Malisetty, R.S., Nair, L. and Rujikiatkamjorn, C. 2024b. Instrumentation and Data Interpretation in Transportation Geotechnics. *Indian Geotechnical Journal*, **54**, 40–62.
Indraratna, B., Qi, Y. & Heitor, A. 2018. Evaluating the properties of mixtures of steel furnace slag, coal wash, and rubber crumbs used as subballast. *Journal of Materials in Civil Engineering,* 30**,** 04017251.
Indraratna, B., Qi, Y. and Rujikiatkamjorn, C. (2025) *Waste Materials Utilisation for Transport Infrastructure.* CRC Press
Indraratna, B., Rujikiatkamjorn, C. & Salim, W. 2023b. *Advanced Rail Geotechnology – Ballasted Track (2nd ed.)*, CRC Press.
Indraratna, B., Rujikiatkamjorn, C., Tawk, M. & Heitor, A. 2019. Compaction, degradation and deformation characteristics of an energy absorbing matrix. *Transportation Geotechnics,* 19**,** 74-83.
Indraratna, B. & Salim, W. 2003. Deformation and Degradation Mechanics of Recycled Ballast Stabilised with Geosynthetics. *Soils and Foundations,* 43**,** 35-46.
Indraratna, B., Salim, W., Ionescu, D. & Christie, D. Stress-strain and degradation behaviour of railway ballast under static and dynamic loading, based on large-scale triaxial testing. Proceedings of the 15th International Confernce on Soil Mechanics and Geotechnical Engineering, 2001 Lisse, Netherlands: A.A. Balkema., 2093-2096.
Indraratna, B., Sun, Y. & Nimbalkar, S. 2016. Laboratory Assessment of the Role of Particle Size Distribution on the Deformation and Degradation of Ballast under Cyclic Loading. *Journal of Geotechnical and Geoenvironmental Engineering,* 142**,** 04016016.
Jayasuriya, C., Indraratna, B. & Ngoc Ngo, T. 2019. Experimental study to examine the role of under sleeper pads for improved performance of ballast under cyclic loading. *Transportation Geotechnics,* 19**,** 61-73.
Kaliboullah, C. I. 2016. *Behaviour of compacted coalwash under saturated condition incorporating particle breakage.* Doctor of Philosophy, University of Wollongong, Australia.
Lackenby, J., Indraratna, B., Mcdowell, G. & Christie, D. 2007. Effect of confining pressure on ballast degradation and deformation under cyclic triaxial loading. *Géotechnique,* 57**,** 527-536.
Malisetty, R. S., Indraratna, B. & Vinod, J. S. 2020a. Multilaminate Mathematical Framework for Analyzing the Deformation of Coarse Granular Materials. *International Journal of Geomechanics,* 20**,** 06020004.
Malisetty, R. S., Indraratna, B. & Vinod, J. S. 2020b. Behaviour of ballast under principal stress rotation: Multi-laminate approach for moving loads. *Computers and Geotechnics,* 125**,** 103655.
Nålsund, R. 2010. Effect of Grading on Degradation of Crushed-Rock Railway Ballast and on Permanent Axial Deformation. *Transportation Research Record,* 2154**,** 149-155.
Navaratnarajah, S. K. & Indraratna, B. 2017. Use of Rubber Mats to Improve the Deformation and Degradation Behavior of Rail Ballast under Cyclic Loading. *Journal of Geotechnical and Geoenvironmental Engineering,* 143**,** 04017015.
Ngo, T., Indraratna, B. & Ferreira, F. 2022. Influence of synthetic inclusions on the degradation and deformation of ballast under heavy-haul cyclic loading. *International Journal of Rail Transportation,* 10**,** 413-435.
Nimbalkar, S. & Indraratna, B. 2016. Improved performance of ballasted rail track using geosynthetics and rubber shockmat. *Journal of Geotechnical and Geoenvironmental Engineering,* 142**,** 04016031.
Noorzad, R. & Raveshi, M. 2017. Mechanical behavior of waste tire crumbs–sand mixtures determined by triaxial tests. *Geotechnical and Geological Engineering,* 35**,** 1793-1802.
Penumadu, D. & Zhao, R. 1999. Triaxial compression behavior of sand and gravel using artificial neural networks (ANN). *Computers and Geotechnics,* 24**,** 207-230.
Phoon, K.-K. & Zhang, W. 2023. Future of machine learning in geotechnics. *Georisk: Assessment and Management of Risk for Engineered Systems and Geohazards,* 17**,** 7-22.
Qi, Y., Indraratna, B., Heitor, A. & Vinod, J. S. 2018. Effect of Rubber Crumbs on the Cyclic Behavior of Steel Furnace Slag and Coal Wash Mixtures. *Journal of Geotechnical and Geoenvironmental Engineering,* 144**,** 04017107.
Rogers, L. L. & Dowla, F. U. 1994. Optimization of groundwater remediation using artificial neural networks with parallel solute transport modeling. *Water Resources Research,* 30**,** 457-481.
Shahin, M. A. & Indraratna, B. 2006. Modeling the mechanical behavior of railway ballast using artificial neural networks. *Canadian Geotechnical Journal,* 43**,** 1144-1152.
Shahin, M. A., Maier, H. R. & Jaksa, M. B. 2002. Predicting Settlement of Shallow Foundations using Neural Networks. *Journal of Geotechnical and Geoenvironmental Engineering,* 128**,** 785-793.
Sheikh, M. N., Mashiri, M. S., Vinod, J. S. & Tsang, H.-H. 2013. Shear and Compressibility Behavior of Sand–Tire Crumb Mixtures. *Journal of Materials in Civil Engineering,* 25**,** 1366-1374.
Sun, Q. D., Indraratna, B. & Nimbalkar, S. 2016. Deformation and Degradation Mechanisms of Railway Ballast under High Frequency Cyclic Loading. *Journal of Geotechnical and Geoenvironmental Engineering,* 142**,** 04015056.
Sun, Y. & Zheng, C. 2017. Breakage and shape analysis of ballast aggregates with different size distributions. *Particuology,* 35**,** 84-92.
Tasalloti, A. 2015. *Behaviour of Blended Waste Materials for Land Reclamation for Port Extension.* Doctor of Philosophy, University of Wollongong, Australia.
Tawk, M. & Indraratna, B. 2021. Role of Rubber Crumbs on the Stress-Strain Response of a Coal Wash Matrix. *Journal of Materials in Civil Engineering,* 33**,** 04020480.
Tennakoon, N. & Indraratna, B. 2014. Behaviour of clay-fouled ballast under cyclic loading. *Géotechnique,* 64**,** 502-506.
Zorlu, K., Gokceoglu, C., Ocakoglu, F., Nefeslioglu, H. & Acikalin, S. 2008. Prediction of uniaxial compressive strength of sandstones using petrography-based models. *Engineering Geology,* 96**,** 141-158.